How to cite: *Angew. Chem. Int. Ed.* **2024**, *63*, e202317102
doi.org/10.1002/anie.202317102

Polymer Chemistry

Cross-domain Chirality Transfer in Self-Assembly of Chiral Block Copolymers

Jun Yuan, Po-Ting Chiu, Xiang Liu, Jiajia Zhou, Yingying Wang, Rong-Ming Ho, and Tao Wen**

Abstract: Chirality transfer is essential to acquire helical hierarchical superstructures from the self-assembly of supramolecular materials. By taking advantage of chirality transfers at different length scales through intra-chain and inter-chain chiral interactions, helical phase (H*) can be formed from the self-assembly of chiral block copolymers (BCPs*). In this study, chiral triblock terpolymers, polystyrene-*b*-poly(ethylene oxide)-*b*-poly(L-lactide) (PS-PEO-PLLA), and polystyrene-*b*-poly(4-vinylpyridine)-*b*-poly(L-lactide) (PS-P4VP-PLLA) are synthesized for self-assembly. For PS-PEO-PLLA with an achiral PEO mid-block that is compatible with PLLA (chiral end-block), H* can be formed while the block length is below a critical value. By contrast, for the one with achiral P4VP mid-block that is incompatible with PLLA, the formation of H* phase would be suppressed regardless of the length of the mid-block, giving cylinder phase. Those results elucidate a new type of chirality transfer across the phase domain that is referred as cross-domain chirality transfer, providing complementary understanding of the chirality transfer at the interface of phase-separated domains.

Introduction

Chirality transfer is a phenomenon widely existing in nature, which is not only related to a variety of chemical and physical processes but also an important process in biological evolution.[1] Self-assembly of chiral motifs can give rise to asymmetric superstructures via homochiral evolution from molecular chirality to conformational chirality and finally hierarchical chirality that thus attracts intensive attention in the past decades.[2] Chirality transfers at different length scales thus give self-assembled phase with helical sense of polymeric materials from molecular level.[3] Twisted lamellae with preferred handedness in the banded spherulites can be formed from the self-assembly of chiral polymers through crystallization.[4] Nanostructures with specific helical sense can be obtained from the self-assembly of chiral block copolymers (BCPs*) through microphase separation, giving rise to the formation of helical phase (H*).[2d,5] Orientational self-consistent field (oSCF) theory has been developed to describe the equilibrium phase behaviors of BCPs* (chiral diblock copolymers) in melt.[6] According to the oSCF theory, the formation of H* is attributed to domain deformation/segment polarization, resulting from segment orientation with inter-chain chiral interaction.[6c] With the enhancement of helical steric hindrance for the inter-chain chiral interaction, the formation window of the H* in phase diagram can be enlarged, as evidenced by introducing the chiral segment with bulky group in diblock for self-assembly with larger twisting power for domain deformation/segment polarization.[7] Moreover, the window of the H* can be enlarged by increasing the segregation strength due to the multiple effects of conformational asymmetry and rod-rod interaction.[8] Accordingly, it is feasible to acquire the H* from the self-assembly of chiral diblock copolymers by varying chemical structures and segregation strength. In contrast to diblock systems, the microphase separation of triblock terpolymers gives rise to additional dimension for the asymmetry effects (composition asymmetry) on self-assembly for twisting in addition to chirality and conformational asymmetry.[9] In our previous work, chiral triblock terpolymers, polystyrene-*b*-PLLA-*b*-poly(D,L-lactide) (PS-PLLA-PLA) and PS-PLA-PLLA were designed and synthesized for self-assembly to examine the effects of the sequence and length of PLLA and PLA segments on the formation of the H* via the domain deformation/segment polarization.[10] Note that the PLLA and PLA blocks are chemically identical except the configuration of chiral centers. Accordingly, PS-PLLA-PLA and PS-PLA-PLLA are referred as two-phase systems, similar to diblock. As found in this study, the inter-chain chiral interaction near the interface of microphase-separated domains is essential to create the twisting and shifting of the domains for the formation of H*.

This work aims to further examine the chirality transfer at the interface of microphase-separated domains through inter-chain chiral interaction by introducing a mid-block to

[*] J. Yuan
Electron Microscopy Center, South China University of Technology
381 Wushan Road, Tianhe District, Guangzhou, 510640 (China)
X. Liu, J. Zhou, Y. Wang, T. Wen
School of Emergent Soft Matter, Guangdong Provincial Key Laboratory of Functional and Intelligent Hybrid Materials and Devices, South China University of Technology
381 Wushan Road, Tianhe District, Guangzhou, 510640 (China)
E-mail: twen@scut.edu.cn
P.-T. Chiu, R.-M. Ho
Department of Chemical Engineering, National Tsing Hua University
101, Section 2, Kuang-Fu Road, Hsinchu, 30013 (Taiwan)
E-mail: rmho@mx.nthu.edu.tw

give triblock terpolymers for self-assembly. Specifically, two types of chiral triblock terpolymers (ABC*), PS-*b*-poly(ethylene oxide)-*b*-PLLA (S–E–LA) and PS-*b*-poly(4-vinylpyridine)-*b*-PLLA (S–V–LA), were designed and synthesized for self-assembly. With a relatively short mid-block, the effect of compositional asymmetry on self-assembly can be alleviated, giving the chiral PLLA end-block as a minor phase in the matrix of the achiral PS end-block. Moreover, with the relatively short mid-block (B), it is possible to form a core–shell phase for triblock terpolymers.[11] Note that the PEO can be compatible with the PLLA while the P4VP is incompatible with the PLLA. As a result, by fine-tuning the compositions and molecular weights of the chiral triblock terpolymer systems, it is feasible to give the formation of the mid-block (PEO or P4VP) shell with chiral PLLA core in achiral PS matrix, providing the represented systems for the examination of the insights of the chirality transfer at the interface of microphase-separated domains. The central theme of this study is to examine the junction effect (midblock effect) on the self-assembly of chiral block copolymers. Our results found that H* can be formed in the S–E–LA while the block length of the PEO is below a critical value. By contrast, there is no H* formation but only cylinder phase in the S–V–LA. Accordingly, the twisting and shifting of the microphase-separated domains indeed requires a new type of chirality transfer across the phase domain that is referred as cross-domain chirality transfer. The corresponding mechanisms may further evidence the conceptual idea with respect to the creation of twisting and shifting, giving the formation of helical superstructures.

Results and Discussion

The chiral triblock terpolymers were synthesized by sequential polymerization of atom transfer radical polymerization (ATRP) or reversible addition-fragmentation chain transfer (RAFT) polymerization, and followed by ring-opening polymerization (ROP) with double-headed initiators. The synthetic routes and procedures of the designed BCPs* were described in detail in the Supporting Information (Schemes S1 and S2, Table S1 in Supporting Information). The volume fraction of P4VP (f_v^{P4VP}), PEO (f_v^{PEO}) and PLLA (f_v^{PLLA}) were calculated by the ^{1}H nuclear magnetic resonance (NMR) (Figures S1–S3), and the molecular weights of PS were determined by gel permeation chromatography (GPC) (Figures S4 and S5). As designed and described, those BCPs possess a relatively short mid-block for alleviation of the effect of compositional asymmetry on self-assembly, giving the chiral PLLA end-block as a minor phase in the matrix of the achiral PS end-block. The compatibility of two polymers can be evaluated by the Flory-Huggins interaction parameter (χ).[12] In this work, the calculated χ values were used when the experimental χ values are not available in the previous reports (Table S3). Based on the prediction of self-consistent field theory (SCFT), the behaviors of self-assembled ABC linear triblock terpolymers can be predicted by the ratios of χ values between segments, $R_1 = \frac{\chi_{AB}}{\chi_{AC}}$ and $R_2 = \frac{\chi_{BC}}{\chi_{AC}}$, and the corresponding volume fractions of the three segments.[11] For S–E–LA, the values of R_1 and R_2 are 0.21 and 0.19, respectively, suggesting that the interactions between two end-blocks are more unfavorable than that of AB and BC contacts. More importantly, the effect of compositional asymmetry from the mid-block on self-assembly should be insignificant due to its low volume fraction. As a result, core–shell cylinders (helical or non-helical) will be expected to form as $f_v^{PS} > 0.3$ and $f_v^{PLLA} < 0.3$.[11] For S–V–LA, the values of R_1 and R_2 are 1.81 and 1.02, respectively. As a result, as the f_v^{P4VP} is below 10 %, core–shell nanostructures are expected to be formed by self-assembly.[13] Accordingly, for all the BCPs* synthesized in this work, the volume fractions would be controlled in the composition range to give the formation of core–shell nanostructures. Figure 1a shows the TEM image of self-assembled S_{48}–E_6–LA_{17} (the subscripts denote the corresponding M_n of each block, see details in Table S1), in which the crescent-like morphology can be observed. The PS microdomain appears dark whereas the PLLA microdomain is bright because of the mass contrast from RuO_4 staining. In addition, the corresponding 1D SAXS profile of the S_{48}–E_6–LA_{17} show well-defined reflections at the relative q values of $1:\sqrt{3}:\sqrt{7}:\sqrt{13}$, indicating that PLLA helices are hexagonally packed in the PS matrix (Figure S6a). Also, the self-assembled nanostructure can be further assured by tilting the TEM specimen, giving clear evidence to distinguish H* from cylinder based on acquired projections with tilting angle. Accordingly, the self-assembled S_{48}–E_6–LA_{17} at the given temperature is identified as an H* phase.

Figure 1b shows the TEM image of self-assembled S_{28}–$V_{5.8}$–LA_{21}; unlike S_{48}–E_6–LA_{17} with H*, there are no peculiar projections but only alternative bright and dark strips can be observed. Moreover, ring-like morphology can be observed in S_{28}–$V_{5.8}$–LA_{21} stained with I_2, confirming the formation of core–shell cylinders (Figure S7). The formation of hexagonally packed PLLA cylinders for S_{28}–$V_{5.8}$–LA_{21} is further evidenced by the corresponding 1D SAXS profiles with the reflections at the relative q values of $1:\sqrt{3}:\sqrt{7}:\sqrt{13}$ (Figure S6b). Note that P4VP microdomains can be selectively stained by I_2. On the basis of the compositions of the S_{28}–$V_{5.8}$–LA_{21}, it is expected to give the formation of core–shell cylinders with P4VP as the shell of PLLA core in PS matrix. As a result, the PEO mid-block of S_{48}–E_6–LA_{17} and

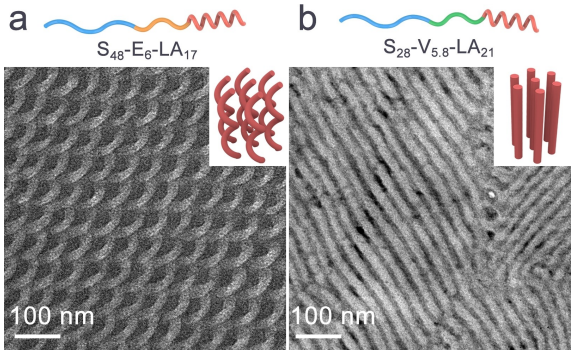

Figure 1. TEM images of self-assembled (a) S_{48}–E_6–LA_{17}; (b) S_{28}–$V_{5.8}$–LA_{21} stained by RuO_4.

P4VP mid-block of S_{28}–$V_{5.8}$–LA_{21} both give rise to the formation of core–shell texture with the mid-block as the shell of PLLA in PS matrix. It is obvious that the existence of the mid-block plays an important role to justify the formation of H* from twisting and shifting of the microdomains.

To further investigate the impact of mid-block on the self-assembly of BCPs*, S–E–LA and S–V–LA with different lengths of mid-blocks were synthesized and examined for self-assembly. Figures 2a and 2b show the TEM images of S_{44}–E_2–LA_{11} and S_{41}–$E_{4.6}$–LA_{21}, respectively, at which the crescent-like morphologies, a typical projection from the H*, can be observed. However, due to the short length of mid-block, it is challenging to observe the intermediate domains of PEO (Figures S8a and S8b). The corresponding 1D SAXS profiles show the reflections at the relative q values of $1:\sqrt{3}:\sqrt{7}$ (Figures S9a and S9b). By contrast, with longer PEO mid-block, i.e., S_{47}–E_{10}–LA_{12}, the self-assembled nanostructures exhibited characteristic morphologies of cylinder phase, rather than H* phase (Figure 2c and Figure S9c). Also, it is found that ring-like morphology can be observed in S_{47}–E_{10}–LA_{12}, resulting from the mass contrast of strained PEO domains (Figure S8c).

Those results indicate that the generation of H* phase in S–E–LA is determined by the length of PEO mid-block. As the M_n^{PEO} of S–E–LA is larger than a critical value, the chirality effect of the self-assembly of BCPs* will be alleviated by the presence of PEO mid-phase. This observation is consistent with our previous results obtained from PS-PLA-PLLA.[10] The critical M_n of PLA mid-block that allows chirality transfer is about 6,000 g/mol in PS-PLA-PLLA,[10] whereas the critical M_n of PEO mid-block in this work is estimated as 8,000 g/mol. For PLA mid-block with M_n of 6,000 g/mol, the spacing of PLA domain in PS-PLA-PLLA can be estimated as $lN^{2/3}=8.1$ nm (where $l=0.423$ nm is the length of a lactoyl repeat unit, and the corresponding degree of polymerization $N=83$).[14] For PEO mid-block with M_n of 8,000 g/mol, the period of PEO domain in PS-PEO-PLLA, can be estimated as $\alpha N^{2/3}=8.9$ nm (where $\alpha=0.278$ nm is the monomer length, and the corresponding degree of polymerization $N=182$).[15] Therefore, we speculate that there is a critical thickness of intermedia domain that allowing chiral transfer in ABC*-type BCPs* with compatible mid-blocks

Figure 2d shows the TEM image of S_{31}–$V_{1.2}$–LA_{17} composed of a mid-block with M_n^{P4VP} of 1,200 g/mol, and the corresponding SAXS profile as shown in Figure S10. These results indicate that H* phase cannot be formed by self-assembly of S–V–LA even with a very short mid-block in the triblock copolymers. Note that it is challenging to observe the intermedia phase by TEM observation due to the reduced length of mid-block (Figure S8d).

As evidenced above, the self-assembly of S–V–LA only gives the formation of cylinder phase, regardless of the length of mid-block, whereas H* phase can be formed by S–E–LA. We speculate that the compatibility of mid-block and chiral block is critical to the self-assembly of chiral triblock terpolymers. To further investigate the observed behaviors, S–E–LA and S–V–LA were examined by DSC. It is found that the glass transition temperature (T_g) of PLLA blocks in S–E–LA decreases with the increase of f_v^{PEO} (Figure S11a), resulting from the high compatibility of PEO and PLLA. In contrast, the T_g of PLLA block in S–V–LA is independent on the length of P4VP mid-block (Figure S11b), confirming that PLLA is indeed incompatible with P4VP in S–V–LA. As a result, in the self-assembly of BCPs* with a mid-block that is compatible with PLLA end-block, e.g., PEO or PLA, the transfer of inter-chain chiral interaction gives rise to the formation of H* phase at which the chirality transfer will be justified by the length of mid-block. By contrast, as the mid-block is incompatible with PLLA, the chirality transfer from chiral end-block to mid-block will be failed, resulting in the non-chiral self-assembly (Figure 3).

On the basis of energetic consideration, the helical steric hindrance at the microphase-separated interface gives the helical curvature, resulting in the twisting of self-assembled

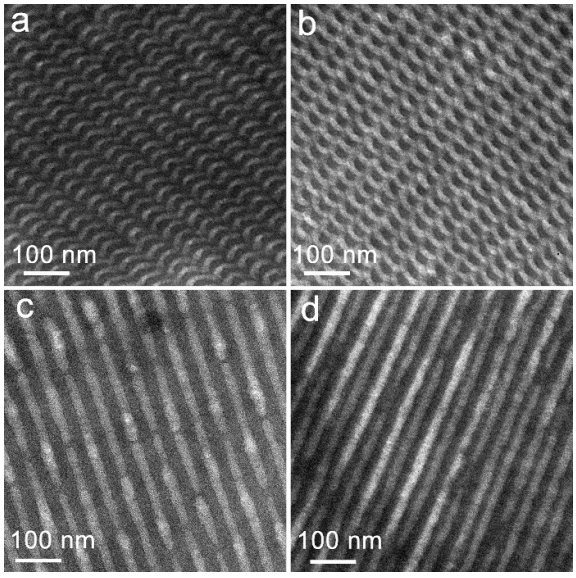

Figure 2. TEM images of self-assembled S_{44}–E_2–LA_{11} (a), S_{41}–$E_{4.6}$–LA_{21} (b), S_{47}–E_{10}–LA_{12} (c), and S_{31}–$V_{1.2}$–LA_{17} (d). Stained by RuO_4.

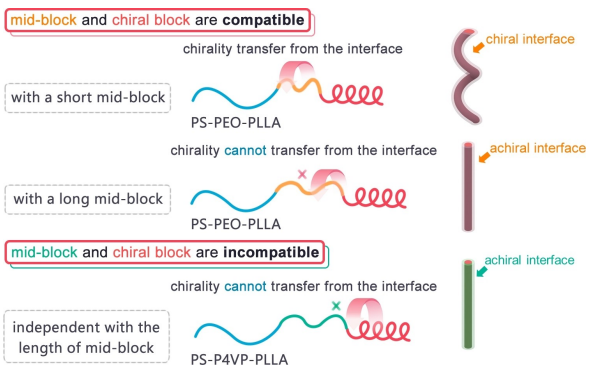

Figure 3. Schematic illustration of chiral transfer in the self-assembly of chiral block copolymers: PS-PEO-PLLA and PS-P4VP-PLLA.

microstructures. The free energy of BCPs* in melt is determined by the mixing enthalpy of unlike segments and the entropic cost to perturb chains from random-walk statistics, as well as the free energy in terms of chiral interactions.[6c] The twisting of a cylinder will increase its surface area under a fixed length, resulting in the increasing of interfacial energy (Figure S12). In particular, there are two interfaces in ABC triblock terpolymers, i.e., A/B and B/C*. As a result, the presence of a mid-block B that is strongly segregated with A and C* blocks will increase the free energy of system once helical structures are formed (see details in SI). In this case, the cross-domain chirality transfer will be alleviated. In contrast, the relatively low interfacial energy in BCPs* with a compatible mid-block allows the formation of helical interface. However, such cross-domain chirality transfer is dependent on the length of mid-block, because the chiral driving force would be dissipated by the long flexible chains.

Conclusion

In summary, cross-domain chirality transfer in the self-assembly of chiral block copolymers was demonstrated by using ABC-type chiral BCPs with a shorter B that can be served as a shell to examine the consequence of microphase-separated interface. As found in this study, the compatibility between mid-block and chiral block is critical to the cross-domain chirality transfer, and thus the formation of helical phase from the mesochiral self-assembly. As mid-block is not compatible with chiral end-block, the high interfacial energy will alleviate the twisting and shifting of PLLA microdomains. In contrast, with a mid-block that is compatible with chiral blocks, chiral interaction gives the formation of core–shell H* phase. This work provides a new insight to the chirality transfer in self-assembly of BCP*.

Acknowledgements

We acknowledge the support from the National Natural Science Foundation of China (21803020), and the Fundamental Research Funds for the Central Universities (2023ZYGXZR107).

Conflict of Interest

The authors declare no conflict of interest.

Data Availability Statement

The data that support the finding of the study are available in the Supporting Information of the article.

Keywords: Block Copolymers · Chirality Transfer · Self-Assembly

[1] T. Wen, H.-F. Wang, M.-C. Li, R.-M. Ho, *Acc. Chem. Res.* **2017**, *50*, 1011.
[2] a) J. H. K. K. Hirschberg, L. Brunsveld, A. Ramzi, J. A. J. M. Vekemans, R. P. Sijbesma, E. W. Meijer, *Nature* **2000**, *407*, 167; b) S. Tomar, M. M. Green, L. A. Day, *J. Am. Chem. Soc.* **2007**, *129*, 3367; c) J. J. L. M. Cornelissen, A. E. Rowan, R. J. M. Nolte, N. A. J. M. Sommerdijk, *Chem. Rev.* **2001**, *101*, 4039; d) R.-M. Ho, Y.-W. Chiang, C.-K. Chen, H.-W. Wang, H. Hasegawa, S. Akasaka, E. L. Thomas, C. Burger, B. S. Hsiao, *J. Am. Chem. Soc.* **2009**, *131*, 18533; e) R.-M. Ho, M.-C. Li, S.-C. Lin, H.-F. Wang, Y.-D. Lee, H. Hasegawa, E. L. Thomas, *J. Am. Chem. Soc.* **2012**, *134*, 10974.
[3] C. Y. Li, S. Z. D. Cheng, J. J. Ge, F. Bai, J. Z. Zhang, I. K. Mann, L.-C. Chien, F. W. Harris, B. Lotz, *J. Am. Chem. Soc.* **2000**, *122*, 72.
[4] a) M.-C. Li, H.-F. Wang, C.-H. Chiang, Y.-D. Lee, R.-M. Ho, *Angew. Chem. Int. Ed.* **2014**, *53*, 4450; b) H.-F. Wang, C.-H. Chiang, W.-C. Hsu, T. Wen, W.-T. Chuang, B. Lotz, M.-C. Li, R.-M. Ho, *Macromolecules* **2017**, *50*, 5466; c) B. Lotz, S. Z. D. Cheng, *Polymer* **2005**, *46*, 577; d) H.-M. Ye, J.-S. Wang, S. Tang, J. Xu, X.-Q. Feng, B.-H. Guo, X.-M. Xie, J.-J. Zhou, L. Li, Q. Wu, G.-Q. Chen, *Macromolecules* **2010**, *43*, 5762; e) J. Xu, S. Zhang, B. Guo, *Chin. Chem. Lett.* **2017**, *28*, 2092.
[5] a) R.-M. Ho, Y.-W. Chiang, C.-C. Tsai, C.-C. Lin, B.-T. Ko, B.-H. Huang, *J. Am. Chem. Soc.* **2004**, *126*, 2704; b) R.-M. Ho, C.-K. Chen, Y.-W. Chiang, B.-T. Ko, C.-C. Lin, *Adv. Mater.* **2006**, *18*, 2355; c) C.-K. Chen, H.-Y. Hsueh, Y.-W. Chiang, R.-M. Ho, S. Akasaka, H. Hasegawa, *Macromolecules* **2010**, *43*, 8637; d) R.-M. Ho, Y.-W. Chiang, S.-C. Lin, C.-K. Chen, *Prog. Polym. Sci.* **2011**, *36*, 376.
[6] a) W. Zhao, T. P. Russell, G. M. Grason, *J. Chem. Phys.* **2012**, *137*, 104911; b) W. Zhao, T. P. Russell, G. M. Grason, *Phys. Rev. Lett.* **2013**, *110*, 058301; c) G. M. Grason, *ACS Macro Lett.* **2015**, *4*, 526.
[7] S. Cai, H. Ma, H. Shi, H. Wang, X. Wang, L. Xiao, W. Ye, K. Huang, X. Cao, N. Gan, C. Ma, M. Gu, L. Song, H. Xu, Y. Tao, C. Zhang, W. Yao, Z. An, W. Huang, *Nat. Commun.* **2019**, *10*, 4247.
[8] K.-C. Yang, P.-T. Chiu, H.-W. Tsai, R.-M. Ho, *Macromolecules* **2021**, *54*, 9850.
[9] M. Liu, W. Li, F. Qiu, A.-C. Shi, *Macromolecules* **2012**, *45*, 9522.
[10] T. Wen, R.-M. Ho, *ACS Macro Lett.* **2017**, *6*, 370.
[11] P. Tang, F. Qiu, H. Zhang, Y. Yang, *Phys. Rev. E* **2004**, *69*, 031803.
[12] a) F. S. Bates, G. H. Fredrickson, *Annu. Rev. Phys. Chem.* **1990**, *41*, 525; b) J. T. Chen, E. L. Thomas, C. K. Ober, G. Mao, *Science* **1996**, *273*, 343; c) F. S. Bates, G. H. Fredrickson, *Phys. Today* **1999**, *52*, 32.
[13] a) C. Auschra, R. Stadler, *Polym. Bull.* **1993**, *30*, 257; b) U. Krappe, R. Stadler, I. Voigt-Martin, *Macromolecules* **1995**, *28*, 4558.
[14] C. A. Joziasse, H. Veenstra, D. W. Grijpma, A. J. Pennings, *Macromol. Chem. Phys.* **1996**, *197*, 2219.
[15] Y. Takahashi, H. Tadokoro, *Macromolecules* **1973**, *6*, 672.

Manuscript received: November 10, 2023
Accepted manuscript online: December 22, 2023
Version of record online: January 12, 2024